

Supporting Information for:

**Highly efficient and stable broadband near-infrared-emitting lead-free metal halide double perovskites**

Guangting Xiong<sup>a</sup>, Lifang Yuan<sup>a, b</sup>, Yahong Jin<sup>a, \*</sup>, Haoyi Wu<sup>a</sup>, Bingyan Qu<sup>c</sup>, Zhenzhang Li<sup>f</sup>, Guifang Ju<sup>a</sup>, Li Chen<sup>a</sup>, Shihe Yang<sup>c, d, \*</sup>, and Yihua Hu<sup>a, \*</sup>

<sup>a</sup> School of Physics and Optoelectronic Engineering, Guangdong University of Technology, Waihuan Xi Road, No. 100, Guangzhou 510006, PR China.

<sup>b</sup> Department Experimental Teaching Department, Guangdong University of Technology, Waihuan Xi Road, No. 100, Guangzhou 510006, PR China.

<sup>c</sup> Institute of Biomedical Engineering, Shenzhen Bay Laboratory, Gaoke International Innovation Center, Guangqiao Road, Guangming District, Shenzhen., PR China.

<sup>d</sup> Guangdong Key Lab of Nano-Micro Material Research, School of Chemical Biology and Biotechnology, Shenzhen Graduate School, Peking University, Shenzhen 518055, PR China.

<sup>e</sup> School of Materials Science and Engineering, Hefei University of Technology, Hefei, Anhui 230009, PR China.

<sup>f</sup> Guangdong Polytechnic Normal University, College of Mathematics and Systems Science, Zhongshan Avenue West, Tianhe District, Guangzhou 510665, PR China.

\*Corresponding author. E-mail: yhjin@gdut.edu.cn; chsyang@pku.edu.cn; huyh@gdut.edu.cn

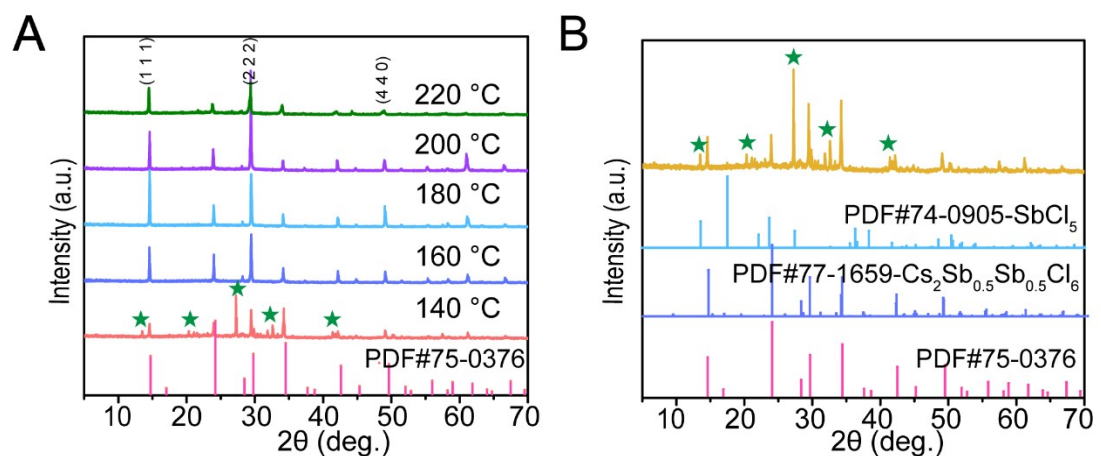


**Fig. S1.** A) XRD patterns  $\text{Cs}_2\text{SnCl}_4\text{Br}_2$ : 0.02Sb prepared at different synthesis temperatures and the standard XRD pattern of  $\text{Cs}_2\text{SnCl}_6$ . B) XRD patterns  $\text{Cs}_2\text{SnCl}_4\text{Br}_2$ : 0.02Sb prepared at 140 °C and the standard XRD patterns of  $\text{Cs}_2\text{Sb}_{0.5}\text{Sb}_{0.5}\text{Cl}_6$  and  $\text{SbCl}_5$ .

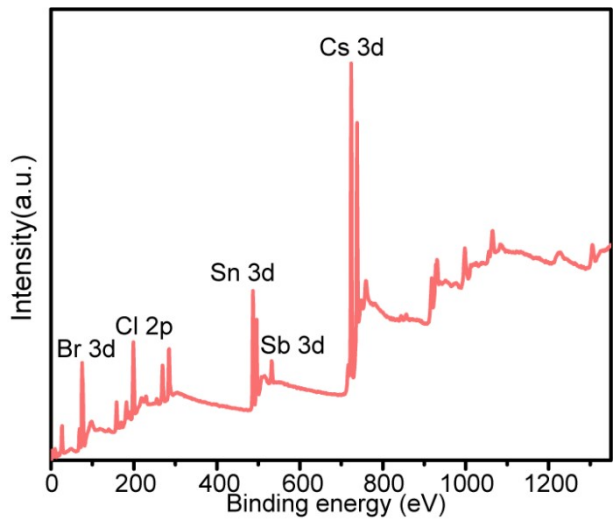


**Fig. S2.** XPS survey spectrum of sample  $\text{Cs}_2\text{SnCl}_4\text{Br}_2$ : Sb.

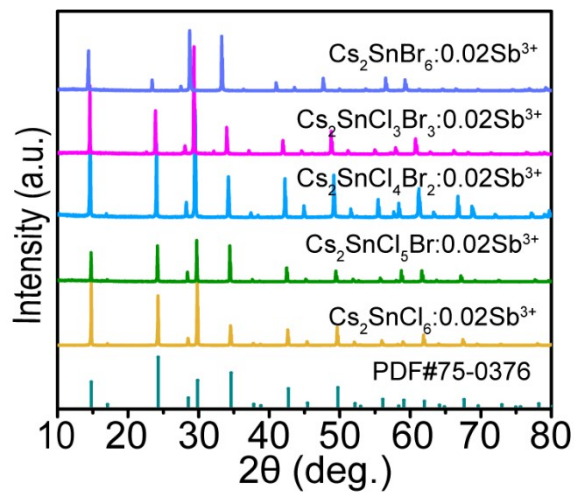


**Fig. S3.** XRD patterns  $\text{Cs}_2\text{SnCl}_x\text{Br}_{6-x}: 0.02\text{Sb}$  ( $x+y=6$ ) and the standard XRD pattern of  $\text{Cs}_2\text{SnCl}_6$  (PDF#75-0376).

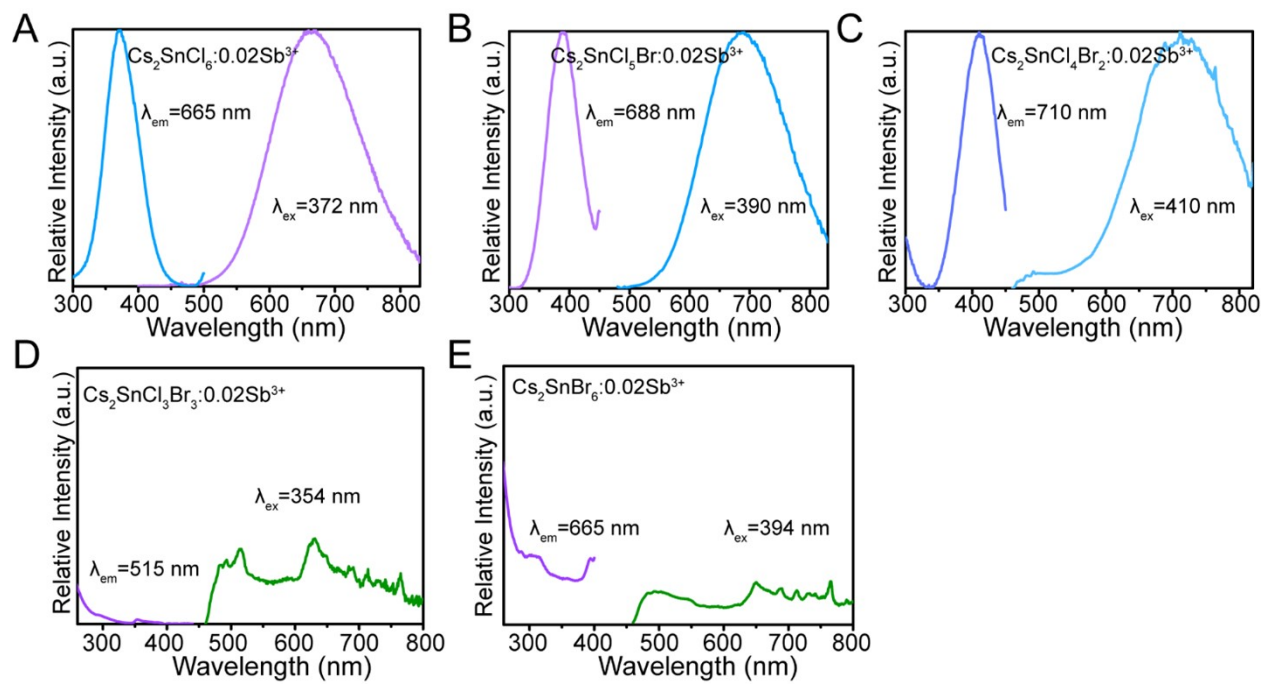


**Fig. S4.** Excitation and emission spectra of the as-synthesized  $\text{Cs}_2\text{SnCl}_x\text{Br}_y \cdot 0.02\text{Sb}^{3+}$  ( $x+y=6$ ) phosphors.

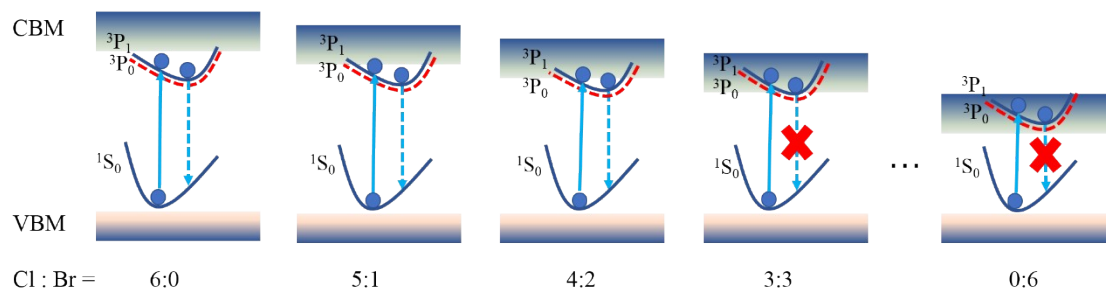


**Fig. S5.** The bandgap and energy level diagram of Sb<sup>3+</sup>-doped Cs<sub>2</sub>SnCl<sub>x</sub>Br<sub>y</sub> (x+y=6).

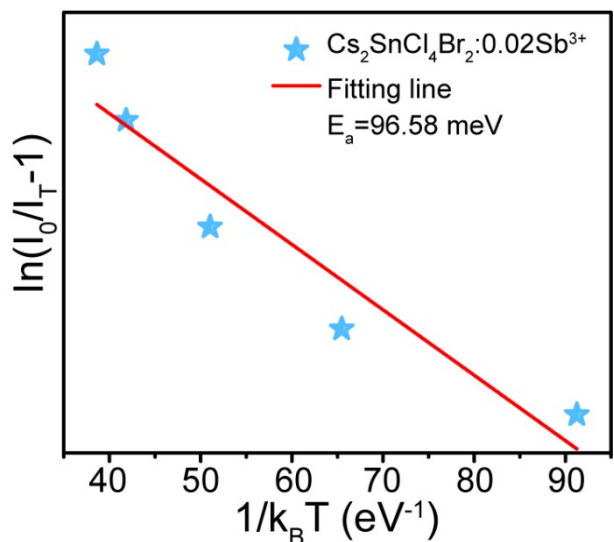


**Fig. S6.** The relationships between  $\ln(I_0/I_T - 1)$  versus  $1/k_B T$  ( $T=77\text{--}300 \text{ K}$ ) and the linear fitting result.

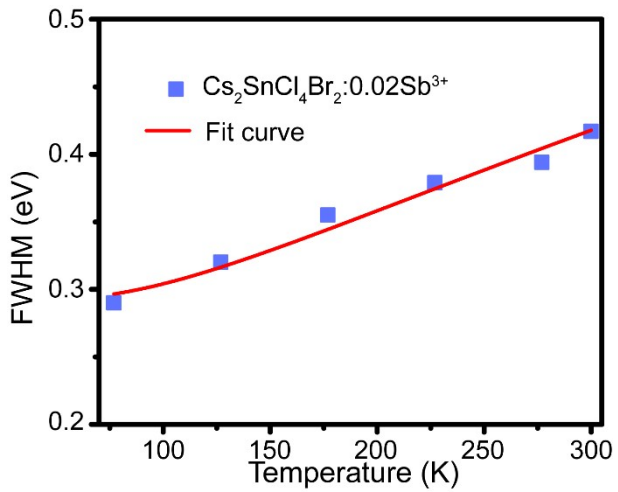


**Fig. S7.** Temperature dependence of PL FWHM of  $\text{Cs}_2\text{SnCl}_4\text{Br}_2$ : 0.02Sb.

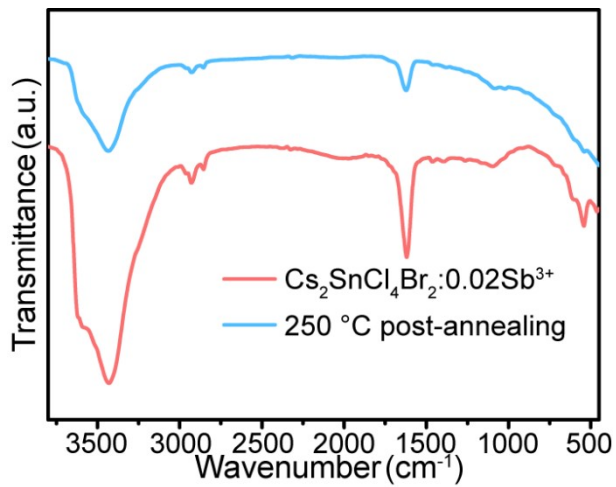


**Fig. S8.** FT-IR of the sample  $\text{Cs}_2\text{SnCl}_4\text{Br}_2$ : 0.02Sb before and after post-annealing at 250 °C.

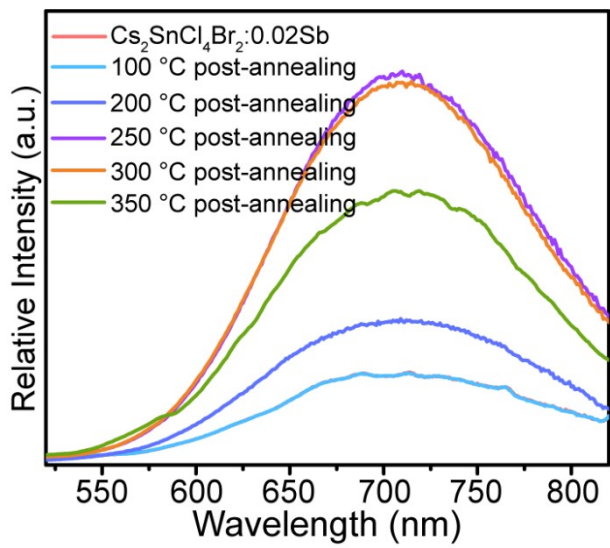


**Fig. S9.** Emission spectra of  $\text{Cs}_2\text{SnCl}_4\text{Br}_2$ : 0.02Sb on post-annealing temperature.

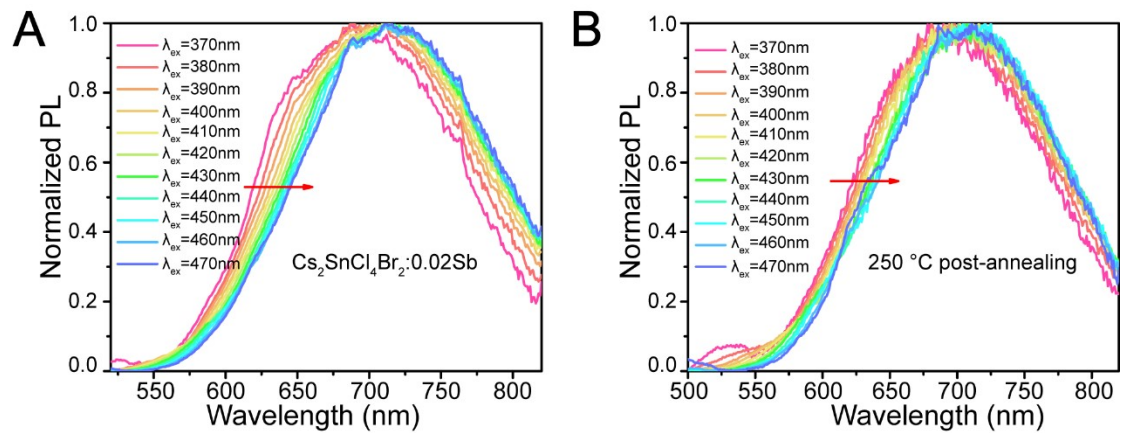


**Fig. S10.** Emission spectra of the original (A) and post-annealed (at 250 °C) (B) sample  $Cs_2SnCl_4Br_2:0.02Sb$  under different excitations varied from 370 to 470 nm.

**Table S1.** The calculated crystallographic data and refinement parameters.

Atoms	Sites	x	y	z	Frac.
Cs1	8c	0.2500	0.2500	0.2500	1.0000
Sn1	4a	0.0000	0.0000	0.0000	1.0000
Cl1	24e	0.2388	0.0000	0.0000	0.7174
Br1	24e	0.2388	0.0000	0.0000	0.3840

**Crystal system:** centric F-centered cubic

**Space group:** Fm-3m

**Z=4**

**Lattice parameters:** a=b=c=10.4663

**Reliable factors:** R<sub>wp</sub>=9.42%, R<sub>p</sub>= 6.67%, χ<sup>2</sup>=3.213

**Table S2.** The chemical composition data of  $\text{Cs}_2\text{SnCl}_4\text{Br}_2$ : 0.02Sb measured by EDS.

Cs (%)	Sn (%)	Cl (%)	Br (%)	Sb (%)	Total atomic (%)
25.85	11.21	49.94	12.66	0.33	100
<b>Theoretical atomic ratio: Cs: Sn: Cl: Br: Sb =2: 1: 4: 2: 0.02</b>					
<b>Experimental ratio: Cs: Sn: Cl: Br: Sb =2.31: 1: 4.45: 1.13: 0.03</b>					

**Table S3.** The summary of PLQY and FWHM of the reported NIR halide perovskites.

	Samples	Emission peaks [nm]	FWHM [nm]	PLQY (%)	Years
Pb-based	$\text{CH}_3\text{NH}_3\text{PbI}_3$	765	50	17	2014 <sup>1</sup>
	$\text{CH}_3\text{NH}_3\text{PbI}_{3-a}\text{Cl}_a$	765	50	30	
	$\text{FAPbI}_3$	770–780	45	>70	2017 <sup>2</sup>
	$\text{CsPbI}_3$	695	50	65	2017 <sup>3</sup>
	$\text{CsSn}_x\text{Pb}_{1-x}\text{I}_3$	700–850	100	0.3–3	2017 <sup>4</sup>
	$\text{Cs}_x\text{FA}_{1-x}\text{PbI}_3$	650–800	50	60–70	2018 <sup>5</sup>
	$\text{PEA}_2\text{Pb}_{1-x}\text{Sn}_x\text{I}_4$	710	154	6	2019 <sup>6</sup>
Pb-free	$\text{CsSn}_x\text{Pb}_{1-x}\text{I}_3:\text{Na}$	830	100	28	2020 <sup>7</sup>
	$\text{MAPbI}_3$	774	50	---	2020 <sup>8</sup>
	$\text{CsSnI}_3$	950	80	0.06	2016 <sup>9</sup>
	$\text{MASnI}_3$	870	85	---	2017 <sup>10</sup>
	{en}MASnI <sub>3</sub>	890	100	---	
	$\text{FASnI}_3$	880	120	---	2019 <sup>11</sup>
	$\text{Cs}_2\text{AgInCl}_6:$	996	50	0.2	2019 <sup>12</sup>
	$\text{Yb/Er}$	1537	60	0.02	
	$\text{Cs}_3\text{Sb}_2\text{I}_9$	750	120	---	2019 <sup>13</sup>
	$\text{Cs}_2\text{AgInCl}_6:\text{Bi/Er}$	1540	50	---	2020 <sup>14</sup>
	$\text{Cs}_2\text{AgInCl}_6:\text{Bi/Yb}$	994	60	---	
$\text{Cs}_2\text{SnCl}_4\text{Br}_2:\text{Sb}$					This work
					14

**Table S4 Photoelectric parameters of the NIR-LEDs fabricated using the samples Cs<sub>2</sub>SnCl<sub>4</sub>Br<sub>2</sub>: 0.02Sb with (NIR-LED-1) and without post-annealing (NIR-LED-2).**

NIR-LEDs	Current (mA)	Voltage (V)	NIR power (mW)	Photoelectric efficiency (%)
NIR-LED-1	19.98	2.95	1.925	3.264
	29.96	2.971	2.887	3.243
	39.97	2.987	3.815	3.195
	49.97	3.003	4.696	3.131
	59.97	3.015	5.564	3.078
	69.98	3.027	6.353	2.999
	79.98	3.039	7.16	2.947
	89.98	3.05	7.882	2.872
	99.99	3.061	8.603	2.811
	149.9	3.112	11.76	2.520
NIR-LED-2	199.9	3.159	14.28	2.261
	250	3.206	16.13	2.012
	299.8	3.25	17.23	1.768
	20	2.945	1.498	2.543
	29.98	2.964	2.261	2.544
	39.98	2.981	3.005	2.521
	49.96	2.995	3.713	2.482
	59.97	3.008	4.396	2.437
	69.97	3.02	5.06	2.395
	79.97	3.032	5.725	2.361
	89.98	3.042	6.328	2.311
	99.99	3.053	6.97	2.283
	149.9	3.102	9.706	2.086
	199.9	3.149	12.05	1.914
	250	3.194	13.85	1.734
	299.9	3.239	15.33	1.578

## References

1. Q. Zhang, S. T. Ha, X. Liu, T. C. Sum, Q. Xiong, Room-temperature near-infrared high-Q perovskite whispering-gallery planar nanolasers. *Nano. Lett.* 14 (2014) 5995-6001.
2. L. Protesescu, S. Yakunin, S. Kumar, J. Bertolotti, N. Masciocchi, A. Guagliardi, M. Grotevent, I. Shorubalko, M. I. Bodnarchuk, Dismantling the "Red Wall" of Colloidal Perovskites: Highly Luminescent Formamidinium and Formamidinium-Cesium Lead Iodide Nanocrystals. *ACS Nano.* 11 (2017) 3119-3134.
3. N. J. L. K. Davis, I. P. a. De, J. Francisco, M. Tabachnyk, J. M. Richter, R. D. Lamboll, E. P. Booker, W. R. R. Florencia, J. T. Griffiths, C. Ducati, S. M, Photon Reabsorption in Mixed  $\text{CsPbCl}_3$ :  $\text{CsPbI}_3$  Perovskite Nanocrystal Films for Light-Emitting Diodes. *J. Phys. Chem. C* 121 (2017) 3790-3796.
4. F. Liu, J.Jiang, C. Ding, Y. Zhang, T. Toyoda, T. S. Ripples, T. Kamisaka, T. Toyoda, S. Hayase, S. Dai, Q. Shen, Colloidal Synthesis of Air-Stable Alloyed  $\text{CsSn}_{1-x}\text{Pb}_x\text{I}_3$  Perovskite Nanocrystals for Use in Solar Cells, *J. Am. Chem. Soc.* 139 (2017) 16708-16719.
5. A. Hazarika, Q. Zhao, E. A. Gaulding, J. A. Christians, B. Dou, A. R. Marshall, T. Moot, J. J. Berry, J. C. Johnson, J. M. Luther, Perovskite Quantum Dot Photovoltaic Materials beyond the Reach of Thin Films: Full-Range Tuning of A-Site Cation Composition, *ACS Nano.* 12 (2018) 10327-10337.
6. J. Yu, J. Kong, W.Hao, X. Guo, H. He, W. R. Leow, Z. Liu, P. Cai, G. Qian, S. Li, X. Chen, X. Chen, Broadband Extrinsic Self-Trapped Exciton Emission in Sn-

Doped 2D Lead-Halide Perovskites, *Adv. Mater.* 31 (2019), 1806385.

7. F. Liu, J. Jiang, Y. Zhang, C. Ding, T. Toyoda, S. Hayase, R. Wang, S. Tao, Q. Shen,

Near-Infrared Emission from Tin-Lead (Sn-Pb) Alloyed Perovskite Quantum Dots by

Sodium Doping, *Angew. Chem.* 132 (2020) 8499-8502.

8. T. Wang, G. Lian, L. Huang, F. Zhu, D. Cui, Q. Wang, Q. Meng, C. Wong,  $\text{MAPbI}_3$

Quasi-Single-Crystal Films Composed of Large-sized Grains with Deep Boundary

Fusion for Sensitive Vis-NIR Photodetectors, *ACS Appl. Mater. Interfaces* 12 (2020)

38314-38324.

9. T. C. Jellicoe, J. M. Richter, H. F. J. Glass, M. Tabachnyk, R. Brady, S. E. Dutton,

A. Rao, R. H. Friend, D. Credgington, N. C. Greenham, Synthesis and Optical

Properties of Lead-Free Cesium Tin Halide Perovskite Nanocrystals, *J. Am. Chem. Soc.* 138 (2016) 2941-2944.

10. W. Ke, C. C. Stoumpos, I. Spanopoulos, L. Mao, M. Chen, M. R. Wasielewski,

M. G. Kanatzidis, Efficient Lead-Free Solar Cells Based on Hollow  $\{\text{en}\}\text{MASnI}_3$

Perovskites, *J. Am. Chem. Soc.* 139 (2017) 14800-14806.

11. X. Meng, J. Lin, X. Liu, X. He, L. Han, Highly Stable and Efficient  $\text{FASnI}_3$ -Based

Perovskite Solar Cells by Introducing Hydrogen Bonding, *Adv. Mater.* 31(2019)

1903721.

12. W. Lee, S. Hong, S. Kim, Colloidal Synthesis of Lead-Free Silver-Indium Double-

Perovskite  $\text{Cs}_2\text{AgInCl}_6$  Nanocrystals and Their Doping with Lanthanide Ions, *J.*

*Phys.Chem. C* 123 (2019) 2665–2672.

13. A. Singh, N.-C. Chiu, K. M. Boopathi, Y.-J. Lu, A. Mohapatra, G. Li, Y.-F.

Chen, T.-F. Guo, C.-W. Chu, Lead-Free Antimony-Based Light-Emitting Diodes through the Vapor-Anion-Exchange Method, ACS Appl. Mater. Interfaces 11 (2019) 35088-35094.

14. H. Arfin, J. Kaur, T. Sheikh, S. Chakraborty, A. Nag, Bi<sup>3+</sup>-Er<sup>3+</sup> and Bi<sup>3+</sup>-Yb<sup>3+</sup> Codoped Cs<sub>2</sub>AgInCl<sub>6</sub> Double Perovskite Near Infrared Emitters, Angew. Chem. Int. Ed. 59 (2020) 11307-11311.